Available online at www.sciencedirect.com
ScienceDirect
Tetrahedron
Tetrahedron 63 (2007) 3585–3590

# Monitoring G-quadruplex structures and G-quadruplex–ligand complex using 2-aminopurine modified oligonucleotides

Takumi Kimura, Kiyohiko Kawai, Mamoru Fujitsuka and Tetsuro Majima*

*The Institute of Scientific and Industrial Research (SANKEN), Osaka University, Mihogaoka 8-1, Ibaraki, Osaka 567-0047, Japan*

Received 27 April 2006; revised 27 June 2006; accepted 27 August 2006
Available online 3 February 2007

**Abstract**—The fluorescent base 2-aminopurine (2Ap) was incorporated into the human telomeric DNA sequence d[AGGG(TTAGGG)$_3$]. The substitution of 2Ap for A in the TTA loops did not affect the G-quadruplex stability. Interestingly, a significant change in the fluorescence intensity of 2Ap between the G-quadruplex and duplex was observed. Therefore, we demonstrated that 2Ap can be used to monitor the duplex to quadruplex conformational change in the human telomeric DNA sequence. This mechanism is explained by the difference in the base stacking in the TTA loop region. Moreover, these probes distinguished between the basket-type and propeller-type G-quadruplexes. We also demonstrated the detection of the telomerase inhibitor agent, such as TMPyP4, using a 2Ap modified telomeric DNA. The formation of the G-quadruplex–ligand complex was observed by the fluorescence titration of TMPyP4.


## 1. Introduction

Telomeres, which are the ends of the linear chromosome of eukaryotes, contain tandem repeats of short G-rich DNA sequences that form structures based on the G-quartet.[1,2] An intramolecular basket-type quadruplex was observed by the folding of the human telomeric sequence, d[AGGG(TTAGGG)$_3$].[3] Half of the Gs possess the *anti* conformation about glycosidic bond, and the other half Gs possess the *syn* conformation. Recent discoveries suggest that telomeres exist in at least two different states or architectures; i.e., 'open' and 'closed' complexes.[4] The 'closed' quadruplex form seems to represent the state that caps and protects the chromosome end. For direct observation of the quadruplex folding, the fluorescence resonance energy transfer (FRET) between the fluorophores attached at each end of the telomeric DNA was measured.[5–7] FRET efficiently occurs in the 'closed' state, in which two fluorophores are in close proximity. In the 'open' structure, the two fluorophores are separated and no FRET is observed. However, a bulky substituent, such as a fluorophore, may inhibit the DNA structural transitions, making it difficult to study the dynamics of the telomeric DNA.[8]

Parkinson et al. reported that DNA oligomers with a human telomeric sequence form not only an intramolecular basket-type G-quadruplex structure, but also an intramolecular propeller-type G-quadruplex structure in the presence of potassium ion.[9] All Gs possess the *anti* conformation, and all four DNA strands are parallel with three linking trinucleotide loops positioned on the exterior of the intramolecular propeller-type G-quadruplex.

The cationic porphyrin, 5,10,15,20-tetrakis(*N*-methyl-4-pyridyl)porphyrin (TMPyP4), has been shown to inhibit telomerase activity in cancer cells.[10] It is known that the complexation of the G-quadruplex-TMPyP4 occurs between a central diagonal loop and the adjacent G-quartet.[11]

The specific properties of DNA structures has been investigated using the fluorescent dye-modified DNA.[12–14] Our previous work demonstrated probing the microenvironment of DNA grooves of B-DNA, A-DNA, and Z-DNA using fluorescence dye, 6-dimethylamino-2-acyl-naphthalene-modified oligomers.[15,16] 2-Aminopurine (2Ap) is a fluorescent adenine isomer able to form a Watson–Crick base pair with T.[17,18] The fluorescence properties of 2Ap in the singlet excited state ($^1$2Ap*) in DNA are strongly influenced by the electron transfer quenching process by G.[19–22] Hence, 2Ap has also been widely employed as a fluorescence probe of the protein-induced local conformational changes in DNA.[23–25] In this study, 2Ap was incorporated into the human telomeric DNA sequences in order to investigate the properties of the G-quadruplex. The fluorescence change of 2Ap in the DNA was observed in the conformational transition of the duplex to the G-quadruplex. Moreover, 2Ap can discriminate between different structures of the G-quadruplex. Subsequently, the binding of TMPyP4 to the G-quadruplex was also detected. On the other hand, no change in the

*Keywords*: G-quadruplex; TMPyP4; Fluorescence probe; DNA conformational transition.
* Corresponding author. Tel.: +81 6 6879 8495; fax: +81 6 6879 8499; e-mail: majima@sanken.osaka-u.ac.jp

0040–4020/$ - see front matter © 2007 Elsevier Ltd. All rights reserved.
doi:10.1016/j.tet.2006.08.108

2Ap fluorescence was observed in the presence of a complementary strand or other porphyrins. These results show that 2Ap probes the specific interaction between the G-quadruplex and TMPyP4.

## 2. Results and discussion

### 2.1. 2Ap in human telomeric DNA detects the conformational transition duplex to the G-quadruplex

To test the possibility of using 2Ap as a probe for the human telomeric quadruplex, we have prepared a set of human telomeric DNA sequences containing a site-specific 2Ap substitution (Fig. 1A, Table 1). First, the effects of the 2Ap substitution on the stability of the G-quadruplex were evaluated by measuring the melting temperature ($T_m$) of the oligodeoxynucleotides (ODNs) by UV thermal denaturation and the CD spectra (Table 1, Fig. 2). The $T_m$ values of the 2Ap modified quadruplexes were not significantly lower than that of the unmodified one. The CD spectra of the 2Ap modified quadruplexes showed two peaks around 240 and 290 nm, and a negative band near 260 nm, which are typical for an anti-parallel quadruplex structure.[26,27] Therefore, the quadruplex can also form in the presence of 2Ap. We then measured the fluorescence intensities for the steady-state fluorescence emission of 2Ap in duplexes ($F_{dup}$) and quadruplexes ($F_{quad}$). An important observation was that $F_{quad}$ was consistently higher than $F_{dup}$ for all the studied sequences. Because π-stacking within the loop by the TTA segments in a quadruplex is highly distorted, the electron transfer quenching of $^1$2Ap* by G in the quadruplex seems to occur less efficiently. In P7 ODN, a significant increase in the fluorescence intensity of 2Ap was over 30-fold for the conformational change from the duplex to the G-quadruplex (Table 1). Interestingly, in the quadruplex form, the fluorescence intensity of 2Ap at the A7 position (P7) was 2–3 times higher than that at the other positions. It is known that the human telomeric quadruplex is stabilized by three stacked G-quartets, which are connected by two lateral loops and a central diagonal loop.[3] Among the four grooves that are formed, one is wide, two are of medium width, and one is narrow. Figure 1B shows that 2Ap at the A7 position of the quadruplex faces one wide and one medium grooves (P7). On the other hand, 2Ap at the A13 (P13) and A19 (P19) positions of the quadruplexes face one narrow and one medium grooves. Therefore, 2Ap at the A7 position is likely to be more hydrated compared with 2Ap at the other positions. Thus, the solvent accessible surface area of 2Ap may also be responsible for the fluorescence properties of 2Ap, since the fluorescence quantum yield of 2Ap is higher in polar solvents.[28,29] To test the microenvironment dependency of the 2Ap fluorescence properties, fluorescence quenching of $^1$2Ap* by the water-soluble antioxidant ascorbic acid[30,31] was investigated. In Figure 3, the ratio $F^0/F$ was plotted versus the concentration of ascorbic acid where $F^0$ and $F$ are the fluorescence intensities of 2Ap in the presence and absence of ascorbic acid as the quencher. The slopes ($K$) of these plots can be assumed to reflect the solvent accessibility of 2Ap. The $K$ values were in the order $P7_{quad} \gg P19_{quad} > P13_{quad} \gg P7_{dup}$. Therefore, 2Ap in the P7 quadruplex is more exposed to solvent than 2Ap at the

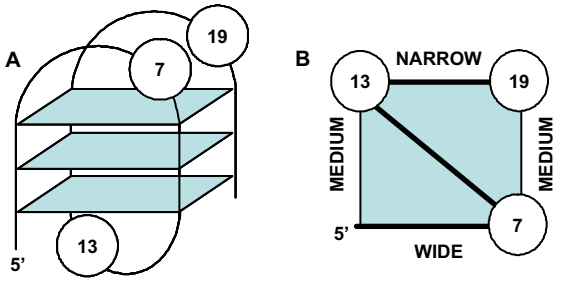


**Figure 1**. (A) Schematic diagram of the human telomeric quadruplex in which the numbers correspond to the positions of As that were individually replaced by Ap in this study. (B) Schematic top view indicating the position of Ap and G-quartet groove widths.

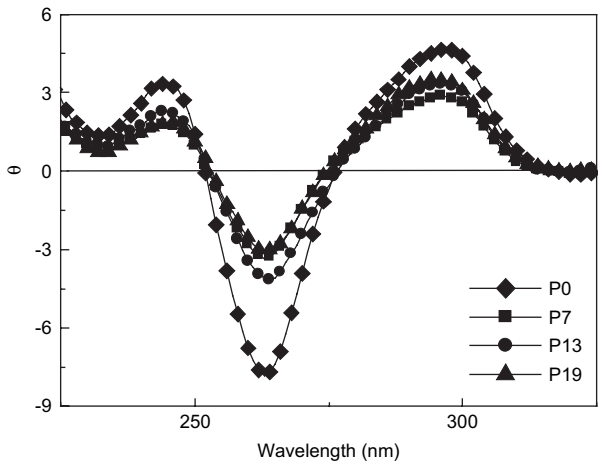


**Figure 2**. CD spectra of the P0, 7, 13, and 19 quadruplexes at 8 °C. Sample solutions contained 100 μM (base concn) ODN, 50 mM sodium-phosphate buffer (pH 7.0), and 100 mM sodium chloride.

**Table 1**. Relative fluorescence intensities[a] at 370 nm ($F$)[b], lifetimes ($t$) and melting temperatures ($T_m$) of 2Ap modified duplexes and G-quadruplexes

| | Sequences | $F_{dup}$[c] | $F_{quad}$ | $K$ ($10^3$ $M^{-1}$) | $\tau_{1(dup)}$ (ns) ($\alpha_1$) | $\tau_{2(dup)}$ (ns) ($\alpha_2$) | $\tau_{1(quad)}$ (ns) | $T_m$[d] (°C) |
|---|---|---|---|---|---|---|---|---|
| P0 | AGGGTTAGGGTTAGGGTTAGGG | | | | | | | 62 |
| P7 | AGGGTT2*Ap*GGGTTAGGGTTAGGG | 1 | 32 | 4.2[e]/0.95[f] | 0.043 (0.82) | 0.64 (0.18) | 0.53 | 56 |
| P13 | AGGGTTAGGGTT2*Ap*GGGTTAGGG | 0.93 | 11 | 2.0[e]/0.88[f] | 0.048 (0.76) | 0.53 (0.24) | 0.34 | 58 |
| P19 | AGGGTTAGGGTTAGGGTT2*Ap*GGG | 1.0 | 13 | 2.4[e]/1.0[f] | 0.052 (0.81) | 0.64 (0.19) | 0.35 | 57 |

[a] Relative fluorescence intensities were evaluated based on the fluorescence intensity of P7 duplex. The fluorescence quantum yields of 2Ap in duplex and quadruplex were up to 0.005 and 0.06, respectively.
[b] Measurement conditions are similar to Figure 2.
[c] 2Ap modified telomeric sequences were hybridized with the complementary DNA strand (5′-CCCTAACCCTAACCCTAACCCT-3′).
[d] Thermal denaturation profiles were recorded using a Jasco V-530 UV–vis spectrophotometer with a thermoelectrical controlled sample holder. Absorbance of the samples was monitored at 260 nm from 2 to 80 °C at a heating rate of 1 °C/min.
[e] Measured for quadruplex structure.
[f] Measured for duplex structure.

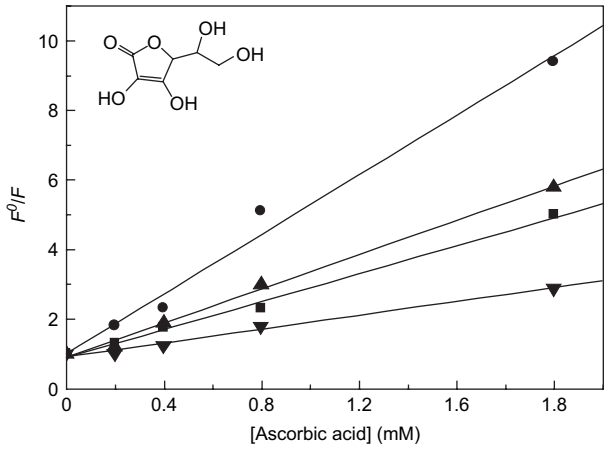


**Figure 3**. Fluorescence quenching of $^1$2Ap* in the quadruplexes and duplex by ascorbic acid. $F_0/F$ was plotted versus the concentration of ascorbic acid, where $F_0$ and $F$ are the fluorescence intensities at 370 nm ($\lambda_{ex}$=300 nm) of Ap in the presence and the absence of ascorbic acid; $P7_{quad}$ (●), $P19_{quad}$ (▲), $P13_{quad}$ (■), $P7_{dup}$ (▼). Sample concentration: 100 μM (base concn) ODN, 50 mM sodium-phosphate buffer (pH 7.0), and 100 mM sodium chloride at 8 °C.

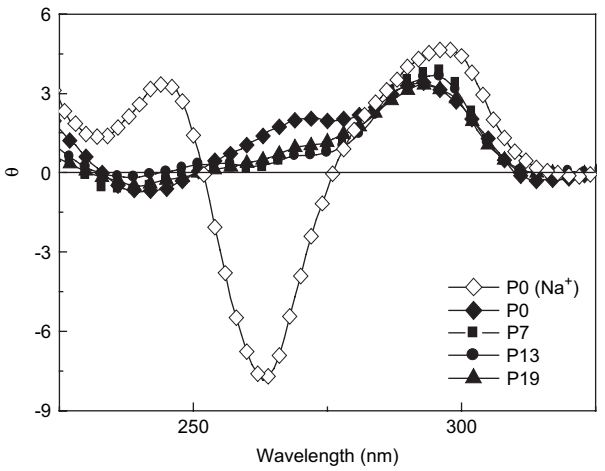


**Figure 4**. CD spectra of the P0, 7, 13, and 19 quadruplexes at 8 °C. Sample solutions contained 100 μM (base concn) ODN, 50 mM potassium cacodylate buffer (pH 6.5), and 100 mM potassium chloride. The condition of P0 ($Na^+$) is similar to Figure 2.

other positions in the quadruplex, or 2Ap in the duplex, resulting in a high fluorescence intensity.

Time-resolved fluorescence measurements with a femtosecond laser were also performed to measure the fluorescence lifetime of $^1$2Ap*, showing results consistent with the steady-state fluorescence measurements. The lifetime of $^1$2Ap* was significantly different in the duplex and quadruplex. In the case of P7 ODN, the lifetime of $^1$2Ap* in the quadruplex ($\tau_{1(quad)}$) was 14-fold longer than that in the duplex ($\tau_{1(dup)}$). The lifetime of $^1$2Ap* in the P7 quadruplex ($\tau_{1(quad)}$) was over 1.5-fold longer than that in the other 2Ap containing quadruplexes. The longer lived components ($\tau_{2(dup)}$) in the duplexes are attributed to the poorly stacked minor conformers.[32]

### 2.2. 2Ap modified telomeric DNA sequences can discriminate between different base stacking in the basket-type and propeller-type structures

It is known that significant changes in the TTA loop orientations occur on the G-quadruplex between the basket-type and propeller-type structures.[9,33] While the basket-type G-quadruplexes have anti-parallel strands, the propeller-type structures have parallel arrangement. Thus, we prepared the 2Ap modified G-quadruplexes in the presence of potassium ion. Regardless of the 2Ap incorporation, the CD spectra displayed positive peaks at 270 and 290 nm, which are typical for a parallel quadruplex structure (Fig. 4).[33] Notably, the fluorescence intensities of the 2Ap modified propeller-type G-quadruplexes were very low compared with that of basket type. The intensity ratios of the propeller type/basket type at the corresponding position of 2Ap were approximately 0.072–0.12 (Table 2). Moreover, fluorescence intensities of the 2Ap modified G-quadruplexes with the propeller-type structure were almost the same. In contrast to the 2Ap fluorescence of the basket-type structure, the propeller type did not depend on the position of 2Ap. The A in each TTA trinucleotide loop of propeller-type structure is swung back so that it intercalates between the two Ts. Jean and Hall

**Table 2**. Relative fluorescence intensities ($F$) of Ap modified telomeric sequences in the presence of sodium or potassium ion

| | Sequences | $F(Na^+)$[a] | $F(K^+)$[b] |
|---|---|---|---|
| P7 | AGGGTT*Ap*GGGTTAGGGTTAGGG | 18 | 1.4 |
| P13 | AGGGTTAGGGTT*Ap*GGGTTAGGG | 9.2 | 1 |
| P19 | AGGGTTAGGGTTAGGGTT*Ap*GGG | 10 | 1.3 |

DNA samples have concentration of 3.6 μM (single strand conc.) at 8 °C.
[a] Sodium chloride of 100 mM, and pH 7, buffered by 5 mM sodium-phosphate solution.
[b] Potassium chloride of 100 mM, and pH 6.5, buffered by 50 mM potassium cacodylate solution.

predicted that 2Ap fluorescence is quenched by stacking with pyrimidines, because of formation of an exciplex between $^1$2Ap* and pyrimidine in a low-lying dark excited state.[34] Therefore, $^1$2Ap* in each TT2Ap loop is quenched by the adjacent Ts. Moreover, the dependency on the position of 2Ap in the propeller-type structure is lower than that of the basket type. This may reflect the fact that the orientation of the three TT2Ap units in these sequences are quite similar. Therefore, 2Ap in the human telomeric DNA can not only monitor the conformational transition of the duplex to the G-quadruplex, but also discriminate between the different base stacking in the basket-type and propeller-type G-quadruplexes.

### 2.3. 2Ap and 7-deazaguanine ($^{dz}$G) modified PZ13 is much more sensitive to TNPyP4 binding to the G-quadruplex

To test the possibility of using 2Ap as a probe for the G-quadruplex–ligand interactions, we used the cationic porphyrin TMPyP4 (Fig. 5) as G-quadruplex-interactive agents to form a specific G-quadruplex–porphyrin complex. TMPyP4 was reported to be a telomerase inhibitor.[10] It is known that TMPyP4 selectively interacts with the G-quadruplex.[11] We prepared a set of 2Ap modified G-quadruplexes (Table 3, P7, P13, and P19). The titration of TMPyP4 into a solution of the 2Ap modified G-quadruplexes showed a relative increase in the 2Ap fluorescence. The estimated saturation concentration of TMPyP4 based on fluorescence titration studies was approximately 4 μM (Fig. 6A). This

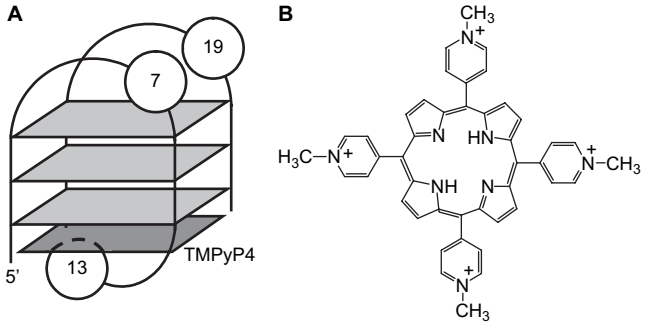


**Figure 5**. (A) Schematic diagram of the G-quadruplex–TMPyP4 complex in which the numbers correspond to the positions of As that were individually replaced by 2Ap in this study. (B) The structure of TMPyP4.

**Table 3**. Sequences and melting temperatures[a] ($T_m$) of the 2Ap modified G-quadruplexes and the 2Ap and $^{dz}$G modified G-quadruplexes

| | Sequences | $T_m$ (°C) |
|---|---|---|
| P0 | AGGGTTAGGGTTAGGGTTAGGG | 62 |
| P7 | AGGGTT2*Ap*GGGTTAGGGTTAGGG | 56 |
| P13 | AGGGTTAGGGTT2*Ap*GGGTTAGGG | 58 |
| P19 | AGGGTTAGGGTTAGGGTT2*Ap*GGG | 57 |
| PZ7 | AGGGTT2*Ap*$^{dz}$*G*GGTTAGGGTTAGGG | 55 |
| PZ13 | AGGGTTAGGGTT2*Ap*$^{dz}$*G*GGTTAGGG | 54 |
| PZ19 | AGGGTTAGGGTTAGGGTT2*Ap*$^{dz}$*G*GG | 54 |

[a] Thermal denaturation profiles were recorded on a Jasco V-530 UV–vis spectrophotometer. Absorbance spectra of the samples were monitored at 260 nm from 10 to 80 °C. DNA samples have concentration of 3.6 μM (single strand concn), sodium chloride of 100 mM, and pH 7, buffered by 5 mM sodium-phosphate solution, at 7 °C.

result indicates that TMPyP4 forms a 1:1 complex with the 2Ap modified G-quadruplex (single strand concn 3.6 μM). Notably, a significant increase in the fluorescence intensity of 2Ap at P13 of the G-quadruplex was observed in the presence of TMPyP4. The fluorescence intensity of 2Ap at P13 was enhanced over 3-fold higher than those at P7 and P19 in the G-quadruplex–TMPyP4 complex. Hurley et al.[35] reported the binding mode of the G-quadruplex–TMPyP4 complex. The complex was constructed by inserting TMPyP4 between a central diagonal loop and G-quartet for d($AG_3[T_2AG_3]_3$), and removing the counter-ion closest to the pyrimidium groups of TMPyP4. Therefore, 2Ap at P13 in the diagonal loop adjacent to the porphyrin may be significantly affected by the TMPyP4 stacking, leading to the increase in the 2Ap fluorescence intensities at P13 because of the decrease in the efficiency of the electron transfer quenching of 2Ap at P13 by neighboring bases (Fig. 5A).

In order to elucidate the denaturation profiles of the G-quadruplex, we performed a fluorescence melting study using the 2Ap modified G-quadruplexes. A melting-induced decrease of the fluorescence intensities of 2Ap in the G-quadruplexes was clearly observed with an increase of the solution temperature (Fig. 6B). Electron transfer quenching of $^1$2Ap* by neighboring G may be enhanced in the linear single strand compared with that in the G-quadruplexes, since distortion of the strand in the G-quadruplexes was relaxed by thermal denaturation to produce an efficient interaction between $^1$2Ap* and the neighboring nucleobases.[36,37]

To design a more sensitive probe of the G-quadruplex–TMPyP4 complex, 7-deazaguanine ($^{dz}$G) was incorporated

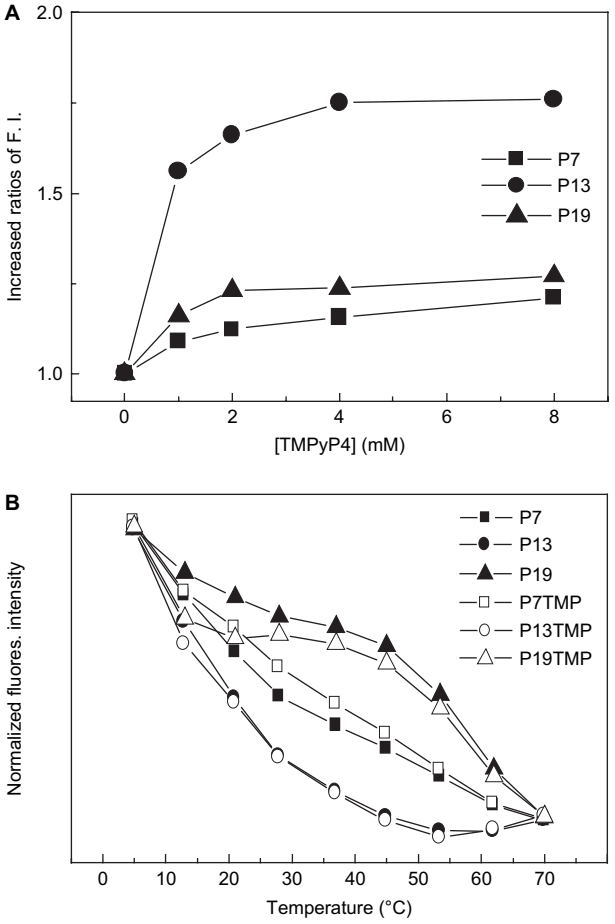


**Figure 6**. (A) Fluorescence titration ($\lambda_{ex}$=305 nm) of the 2Ap modified G-quadruplex; P7, P13, and P19 with TMPyP4 (0, 1, 2, 4, and 8 μM). DNA samples have concentration of 3.6 μM (single strand concn), sodium chloride of 100 mM, and pH 7, buffered by 50 mM sodium-phosphate solution at 5 °C in the following conditions. (B) Thermal melting profiles of the 2Ap modified G-quadruplexes. Fluorescence of the samples was monitored at 370 nm, from 5 to 70 °C.

into the G-quartet adjacent to 2Ap (Table 1, PZ7, PZ13, and PZ19). $^{dz}$G has a much lower oxidation potential than G, and is expected to amplify the effects of electron transfer during the 2Ap fluorescence quenching.[22] First, effects of the $^{dz}$G substitution on the stability of the G-quadruplexes were examined by measuring $T_m$ and CD spectra (Fig. 7). The results showed that the $^{dz}$G substitution does not significantly destabilize the G-quadruplex structure. The incorporation of $^{dz}$G resulted in a decreased fluorescence intensity of 2Ap, showing that $^1$2Ap* was efficiently quenched by $^{dz}$G (Fig. 8A). Therefore, we confirmed that the fluorescence intensity of 2Ap in the loop of the G-quadruplex is affected by the G-quartet. The titration of TMPyP4 into a solution of PZ13 resulted in approximately 2.5-fold increase in the fluorescence intensity of 2Ap, showing that PZ13 serves as a better probe than P13. In contrast, as for the other $^{dz}$G substituted ODNs (PZ7 and PZ19), the fluorescence intensity of 2Ap was not affected by the presence of TMPyP4 (Fig. 8B). Thus, the results clearly demonstrate that the increase in the fluorescence intensity of 2Ap is due to the TMPyP4 binding between the diagonal loop and adjacent G-quartet.

In order to examine the ability of PZ13 to detect the G-quadruplex–TMPyP4 complex formation, fluorescence titration

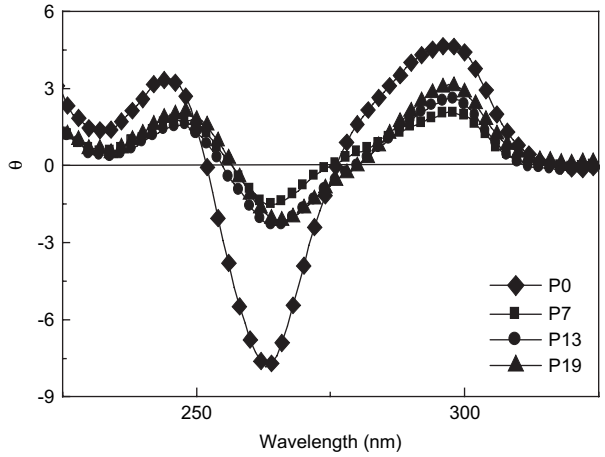


**Figure 7**. CD spectra of the P0, 7, 13, and 19 quadruplexes at 8 °C. Sample solutions contained 100 μM (base concn) ODN, 50 mM sodium-phosphate buffer (pH 7.0), and 100 mM sodium chloride.

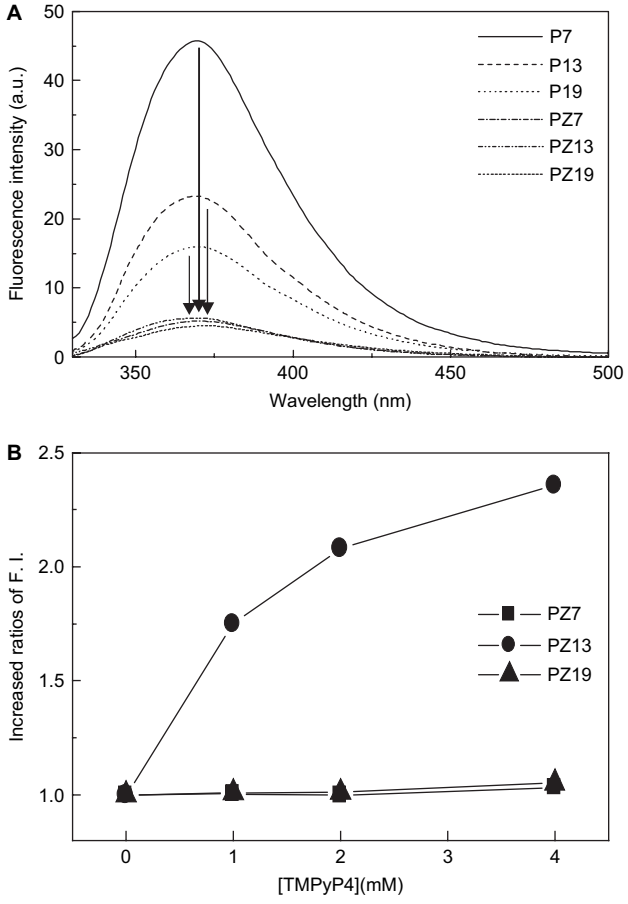


**Figure 8**. (A) Fluorescence spectra of the 2Ap modified G-quadruplexes and the 2Ap and $^{dz}$G modified G-quadruplexes. (B) Fluorescence titration of the 2Ap and $^{dz}$G modified G-quadruplex; PZ7, PZ13, and PZ19 with TMPyP4 (0, 1, 2, and 4 μM).

experiments were performed with a number of transition-metal complexes of porphyrins (5,10,15,20-tetrakis(4-methoxyphenyl)-21H,23H-porphyrin cobalt(II)—TMP-Co and 5,10,15,20-tetrakis(pentafluorophenyl)porphyrin iron(III)—TPP-Fe). In results, no change in the 2Ap fluorescence was observed in the presence of the transition-metal porphyrin complexes (Fig. 9). The fluorescence intensity of 2Ap was

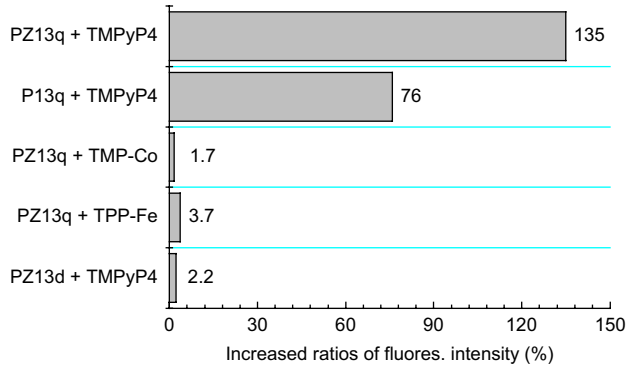


**Figure 9**. Specific recognition of TMPyP4 by PZ13 G-quadruplex (PZ13q). The concentrations of free and metal porphyrins (TMPyP4, TMP-Co, and TPP-Fe) are 4 mM. PZ13d is hybridized with the complementary strand.

also unaffected by the addition of TMPyP4 when PZ13 forms a duplex (PZ13d) with the complementary strand. These results clearly showed that PZ13 can be used for the detection of the G-quadruplex–TMPyP4 complex.

## 3. Conclusions

In this study, our results showed that 2Ap can be used to monitor the duplex to quadruplex conformational change of the human telomeric DNA sequence. The substitution of 2Ap for A7 in the sequence was effective for the detection of conformational transition. Therefore, fluorescence properties of 2Ap in G-quadruplexes depended on the base-stacking interactions and solvent accessibility. The human telomeric DNA has two G-quadruplex structures such as basket type or propeller type. We also demonstrated that 2Ap can recognize these two structures. The fluorescence intensity of 2Ap in the propeller-type structure was lower than that of basket-type one. These results are explained by the differences of the base stacking of TT2Ap trinucleotide loops of G-quadruplexes. In propeller-type G-quadruplex, the fluorescence quenching of 2Ap occurs by intercalating between two Ts. Moreover, the fluorescence intensities of 2Ap in this G-quadruplexes were closely similar because of widths of four phosphate grooves and the orientations of three protruding loops are equivalent.

The specific complex formation of G-quadruplex and TMPyP4 could be effectively monitored by the 2Ap and $^{dz}$G modified human telomere sequences. This detection method of telomerase inhibitor is based on the quenching inhibition with the G-quadruplex–ligand interaction. The increase in the fluorescence intensity of 2Ap is due to the TMPyP4 binding between the diagonal loop and the adjacent G-quartet. These probes are not only useful to provide information about the G-quadruplex structures, but also detect the G-quadruplex–TMPyP4 complex formation. It will be useful for studying the biological role of the G-quadruplexes.

## 4. Experimental

### 4.1. Preparation of oligonucleotides

Phosphoramidite monomers and 2-aminopurine-CE-phosphoramidite were purchased from Glen Research Co., Ltd.

ODNs were synthesized on an Expedite 8909 DNA synthesizer (Applied Biosystems) in the 1.0 μM scale. After the automated synthesis, the ODNs were treated with aqueous ammonia solution overnight at 40 °C. Crude ODNs were purified by reverse phase HPLC and lyophilized. Purity and concentrations of all ODNs were determined by complete digestion with snake venom PDE, nuclease P1, and alkali phosphatase enzymes to 2′-deoxymononucleosides.

### 4.2. CD, fluorescence, and UV measurement

The circular dichroism (CD) spectra were recorded using a Jasco J-700 spectrophotometer. The CD spectra of the ODN solutions were recorded 1 nm steps (sensitivity 5 mdeg; band width 2 nm; scanning rate 50 mV/s) from 320 to 230 nm by using an 1 cm path length cell at 2 °C. Fluorescence spectra were measured on a Hitachi 850 spectrofluorometer. Ultraviolet (UV) spectra were recorded with a JASCO V-530 spectrophotometer.

### 4.3. Time-resolved fluorescence spectral measurement

Time-resolved fluorescence spectra were measured by the single photon counting method using a streakscope (Hamamatsu Photonics, C4334-01) equipped with a polychromator (Acton Research, SpectraPro150). Ultrashort laser pulse was generated with a Ti:sapphire laser (Spectra-physics, Tsunami 3941-M1BB, FWHM 100 fs) pumped with a diode-pumped solid state laser (Spectra-physics, Millennia VIIIs). For excitation of the sample, the output of the Ti:sapphire laser was converted to third harmonic generation (300 nm) with a harmonic generator (Spectra-physics, GWU-23FL). The emission was monitored with a streak camera at wavelength 370 nm. The more details about measurement method has been previously reported.[38–40]

## Acknowledgements

This work has been partly supported by a Grant-in-Aid for Scientific Research (Project 17105005, Priority Area (417), 21st Century COE Research, and others) from the Ministry of Education, Culture, Sports, Science and Technology (MEXT) of Japanese Government.

## References and notes

1. Zakian, V. A. *Annu. Rev. Genet.* **1989**, *23*, 579–604.
2. Blackburn, E. H. *Nature* **1991**, *350*, 569–573.
3. Wang, Y.; Patel, D. J. *Structure* **1993**, *1*, 263–282.
4. Zahler, A. M.; Williamson, J. R.; Cech, T. R.; Prescott, D. M. *Nature* **1991**, *350*, 718–720.
5. Darby, R. A. J.; Sollogoub, M.; McKeen, C.; Brown, L.; Risitano, A.; Brown, N.; Barton, C.; Brown, T.; Fox, K. R. *Nucleic Acids Res.* **2002**, *30*, e39/1–e39/8.
6. Ying, L.; Green, J. J.; Li, H.; Klenerman, D.; Balasubramanian, S. *Proc. Natl. Acad. Sci. U.S.A.* **2003**, *100*, 14629–14634.
7. Alberti, P.; Mergny, J.-L. *Proc. Natl. Acad. Sci. U.S.A.* **2003**, *100*, 1569–1573.
8. Green, J. J.; Ying, L.; Klenerman, D.; Balasubramanian, S. *J. Am. Chem. Soc.* **2003**, *125*, 3763–3767.
9. Parkinson, G. N.; Lee, M. P. H.; Neidle, S. *Nature* **2002**, *417*, 876–880.
10. Wheelhouse, R. T.; Sun, D.; Han, H.; Han, F. X.; Hurley, L. H. *J. Am. Chem. Soc.* **1998**, *120*, 3261–3262.
11. Han, F. X.; Wheelhouse, R. T.; Hurley, L. H. *J. Am. Chem. Soc.* **1999**, *121*, 3561–3570.
12. Johansson, M. K.; Fidder, H.; Dick, D.; Cook, R. M. *J. Am. Chem. Soc.* **2002**, *124*, 6950–6956.
13. Okamoto, A.; Tainaka, K.; Nishiza, K.-i.; Saito, I. *J. Am. Chem. Soc.* **2005**, *127*, 13128–13129.
14. Pal, S. K.; Zhao, L.; Xia, T.; Zewail, A. H. *Proc. Natl. Acad. Sci. U.S.A.* **2003**, *100*, 13746–13751.
15. Kimura, T.; Kawai, K.; Majima, T. *Org. Lett.* **2005**, *7*, 5829–5832.
16. Kimura, T.; Kawai, K.; Majima, T. *Chem. Commun.* **2006**, 1542–1544.
17. McLaughlin, L. W.; Leong, T.; Benseler, F.; Piel, N. *Nucleic Acids Res.* **1988**, *16*, 5631–5644.
18. Law, S. M.; Eritja, R.; Goodman, M. F.; Breslauer, K. J. *Biochemistry* **1996**, *35*, 12329–12337.
19. Kelley, S. O.; Barton, J. K. *Science* **1999**, *283*, 375–381.
20. Lewis, F. D.; Letsinger, R. L.; Wasielewski, M. R. *Acc. Chem. Res.* **2001**, *34*, 159–170.
21. Tashiro, R.; Sugiyama, H. *Angew. Chem., Int. Ed.* **2003**, *42*, 6018–6020.
22. Kimura, T.; Kawai, K.; Fujitsuka, M.; Majima, T. *Chem. Commun.* **2004**, 1438–1439.
23. Petrauskene, O. V.; Schmidt, S.; Karyagina, A. S.; Nikolskaya, I. I.; Gromova, E. S.; Cech, D. *Nucleic Acids Res.* **1995**, *23*, 2192–2197.
24. Malygin, E. G.; Zinoviev, V. V.; Petrov, N. A.; Evdokimov, A. A.; Jen-Jacobson, L.; Kossykh, V. G.; Hattman, S. *Nucleic Acids Res.* **1999**, *27*, 1135–1144.
25. Dunlap, C. A.; Tsai, M.-D. *Biochemistry* **2002**, *41*, 11226–11235.
26. Miyoshi, D.; Nakao, A.; Toda, T.; Sugimoto, N. *FEBS Lett.* **2001**, *496*, 128–133.
27. Balagurumoorthy, P.; Brahmachari, S. K. *J. Biol. Chem.* **1994**, *269*, 21858–21869.
28. Rachofsky, E. L.; Osman, R.; Ross, J. B. A. *Biochemistry* **2001**, *40*, 946–956.
29. Frei, B.; England, L.; Ames, B. N. *Proc. Natl. Acad. Sci. U.S.A.* **1989**, *86*, 6377–6381.
30. Podmore, I. D.; Griffiths, H. R.; Herbert, K. E.; Mistry, N.; Mistry, P.; Lunec, J. *Nature* **1998**, *392*, 559–562.
31. Gramlich, G.; Zhang, J.; Nau, W. M. *J. Am. Chem. Soc.* **2002**, *124*, 11252–11253.
32. Larsen, O. F. A.; Van Stokkum, I. H. M.; Gobets, B.; Van Grondelle, R.; Van Amerongen, H. *Biophys. J.* **2001**, *81*, 1115–1126.
33. Li, W.; Wu, P.; Ohmichi, T.; Sugimoto, N. *FEBS Lett.* **2002**, *526*, 77–81.
34. Jean, J. M.; Hall, K. B. *Biochemistry* **2002**, *41*, 13152–13161.
35. Han, H.; Langley, D. R.; Rangan, A.; Hurley, L. H. *J. Am. Chem. Soc.* **2001**, *123*, 8902–8913.
36. Xu, D.-G.; Nordlund, T. M. *Biophys. J.* **2000**, *78*, 1042–1058.
37. Abdou, I. M.; Sartor, V.; Cao, H.; Schuster, G. B. *J. Am. Chem. Soc.* **2001**, *123*, 6696–6697.
38. Fujitsuka, M.; Hara, M.; Tojo, S.; Okada, A.; Troiani, V.; Solladie, N.; Majima, T. *J. Phys. Chem. B* **2005**, *109*, 33–35.
39. Oseki, Y.; Fujitsuka, M.; Cho, D. W.; Sugimoto, A.; Tojo, S.; Majima, T. *J. Phys. Chem. B* **2005**, *109*, 19257–19262.
40. Cho, D. W.; Fujitsuka, M.; Choi, K. H.; Park, M. J.; Yoon, U. C.; Majima, T. *J. Phys. Chem. B* **2006**, *110*, 4576–4582.